International Journal of Applied Sciences & Engineering (IJASE) **2**(1) : April 2014, 1-12

DOI No. 10.5958/2322-0465.2014.01112.5

Influence of Fiber Volume Fraction, Fiber Angle and Hole Size on the Stress Concentration around the Circular Hole of an Orthotropic Lamina under unidirectional in Plane Loading

Chaitanya Goteti* and Sreenivasulu Reddy

Department of Mechanical Engineering, R.V.R and J.C College of Engineering, Guntur, A.P, India.

*Corresponding author: Chaitanya Goteti; chaitanyagoteti16@gmail.com

ABSTRACT

This work examines the effect of fiber angle, fiber volume fraction and hole size on the stress concentration around the circular hole of (AS4/3501-6) carbon/Epoxy lamina subjected to unidirectional in plane loading. Three independent fiber volume fractions and fiber orientations for three different hole sizes are considered. Both analytical and finite element solutions are presented using micro and macro mechanics approaches of analysis of orthotropic lamina and by using ANSYS10 finite element package. The analysis is initially carried out by fixing the hole size and by varying the other two parameters (fiber angle and fiber volume fraction). Next, the fixing parameter is interchanged in a cyclic fashion and the process is continued. It is found that the whole size and fiber orientation have greater influence on the stress intensity concentration around the hole vicinity compared to fiber volume fraction.

Keywords: Fiber angle, volume fraction, stress concentration, hole size

Carbon/epoxy continuous fiber composite laminates are in use as structural elements or as supporting elements for different structures due to their high strength and stiffness. The bolt holes drilled to join the structural elements cause stress concentration problems as in case of metallic members. Unlike metals, the laminate material properties in the loading direction depend on the fiber orientation and fiber volume fraction. Hence, these two parameters are of interest to designers. B.T. Astrom (1992) presented various manufacturing methods like Resin transfer molding, Autoclave molding...etc in detail for polymer matrix composites. P.K. Mallick (1993) gave a detailed and in depth information on materials, property characterization, testing and various methods of manufacture of fiber reinforced composites. Bhagwan

D.Agarwal *et al.,* (2006) presented clear and elaborative information on manufacturing, characterization and failure behavior of fiber reinforced composite materials. The semi empirical relation for transverse elastic modulus as a function of fiber volume fraction for unidirectional FRP composites was given by Halpin and Tsai (1967). Halpin (1969) presented a semi empirical relation to determine the longitudinal elastic modulus of FRP composites as a function of fiber volume fraction, matrix modulus and fiber modulus. Z. Hashin (1983) developed a semi empirical relation for transverse elastic modulus of FRP laminates as a function of bulk modulus and transverse shear modulus of laminate based on solid mechanics approach. O. Ishai (1971) analyzed the transverse micro cracking of glass/epoxy laminate under unidirectional tensile loading. A theory based on stress tensors for predicting the failure behavior of composites under tension and compression was proposed by S.W. Tsai and E.M Wu (1971). C.T Sun (2000) reviewed different failure theories and showed comparisons of theoretical predictions with experimental results for various composite material systems under different loading conditions. I.M.Daniel *et al.,* (1974) analyzed the effect of material and layer stacking sequence on the stress distribution around the holes of boron/epoxy laminates. H.J. Konish and J.M. Whitney (1975) presented an approximate relation for stress distribution along the in plane transverse axis of the circular hole of an orthotropic plate subjected to loading in longitudinal direction. R.J. Nuismer and J.M. Whitney (1975) presented a relation to estimate the stress concentration factor for holed orthotropic plates subjected to uniaxial in plane loading based on laminate stffnesses. R.F. Karlak (1977) analyzed the effect of hole size on the stress distributions in various symmetrically stacked laminates. I.M. Daniel (1982) studied the failure of composite laminates due to stress concentration around the holes of various sizes and on through thickness cracks. J. Awerbuch and M.S. Madhukar (1985) presented an elaborative review on various theoretical and experimental results on stress concentrations in notched composite laminates. In the present work, the lamina properties for (AS-4/3501-6) carbon/epoxy composite along and transverse to fiber directions for three different fiber volume fractions ($V_f = 0.75$, $V_f = 0.5$ and $V_f = 0.25$) are found based on the chosen matrix and fiber properties and by implementing rule of mixtures and Halpin-Tsai semi empirical relations. The lamina properties along and transverse to the loading direction for three fiber angles (θ = 0deg, θ = 45deg and θ = 90deg) are found by using the transformation relations. The stress intensity around the circumference of the circular hole for three different hole sizes (D = 10mm, D = 20mm and D = 30mm) is estimated using the R.J. Nuismer and H.J. Konish approximate relations. Using the layered shell elements, the finite element analysis for the three different hole sizes with varying fiber angles and fiber volume fractions is carried out and the results are compared with the theoretical results. A good congruence is found between the theoretical and finite element results.

Table 1: Mechanical properties of carbon fibers and epoxy resin matrix

Property	As4-Carbon Fiber	3501-6 Epoxy resin matrix
Modulus of Elasticity	235 Gpa (Along fiber length)	4.3 Gpa
Modulus of Elasticity	15 Gpa (Normal to fiber Length)	
Shear Modulus	27 Gpa (In plane 1-2)	1.6 Gpa
Shear Modulus	7 Gpa (In plane 2-3)	
Poisson's Ratio (Major)	0.2	0.35

Theoretical Analysis

The fiber and matrix properties related to AS4/3501-6 carbon/epoxy lamina are shown in Table 1.

Following the principle of rule of mixtures and semi empirical relations given by Halpin-Tsai, the properties of the composite such as elastic modulus, shear modulus and Poisson's ratio along the fiber direction and transverse to the fiber direction are derived as shown.

$$E_1 = V_f \times E_{1f} + V_m \times E_m \quad \text{(Rule of mixtures)} \tag{1}$$

Where $V_f + V_m = 1$ (Assuming zero void volume fraction) (2)

$$E_2 = E_m\left(\frac{1+\xi\eta V_f}{1-\eta V_f}\right) \quad \text{(Halpin-Tsai Semi Empirical Relation)} \tag{3}$$

Where $\xi = 1$ (For carbon and boron epoxy laminates) $\eta = \left(\frac{E_{2f} - E_m}{E_{2f} + \xi E_m}\right)$ (4)

$$G_{12} = G_m \times \left(\frac{1+\xi\eta V_f}{1-\eta V_f}\right) \quad \text{(Halpin-Tsai Semi Empirical Relation)} \tag{5}$$

$$\eta = \left(\frac{G_{12f} - G_m}{G_{12f} + \xi G_m}\right) \tag{6}$$

$$\frac{\upsilon_{12}}{E_1} = \frac{\upsilon_{21}}{E_2} \quad \text{(Betti's Reciprocal law)} \tag{7}$$

The properties of carbon/epoxy composite lamina along and transverse to fiber direction derived from the equations 1 to 7 for the three different fiber volume fractions (V_f=0.75, V_f=0.5 and V_f=0.25) are tabulated in Table 2 as shown.

Table 2: Mechanical properties of Lamina for different fiber volume fractions

Property	Volume Fractions		
	V_f=0.75	V_f=0.5	V_f=0.25
Elastic Modulus (E_1)	177.325 (Gpa)	119.65 (Gpa)	61.975 (Gpa)
Elastic Modulus (E_2)	10.413 (Gpa)	7.594 (Gpa)	5.6825 (Gpa)
Shear Modulus (G_{12})	7.980 (Gpa)	4.155 (Gpa)	2.513 (Gpa)
Major Poisson's Ratio (υ_{12})	0.2375	0.275	0.3125
Minor Poisson's Ratio (υ_{21})	0.01394	0.01745	0.02865

The properties of the composite lamina parallel and perpendicular to the loading direction (parallel and perpendicular to the plate geometrical axes) are obtained using the following transformation relations.

$$\frac{1}{E_x}=\frac{c\cos^2\theta}{E_1}\left(c\cos^2\theta-\sin^2\theta\upsilon_{12}\right)+\frac{sin^2\theta}{E_2}\left(\sin^2\theta-c\cos^2\theta\upsilon_{21}\right)+\frac{\cos^2\theta\sin^2\theta}{G_{12}} \tag{8}$$

$$\frac{1}{E_y}=\frac{sin^2\theta}{E_1}\left(\sin^2\theta-c\cos^2\theta\upsilon_{12}\right)+\frac{c\cos^2\theta}{E_2}\left(c\cos^2\theta-\sin^2\theta\upsilon_{21}\right)+\frac{\cos^2\theta\sin^2\theta}{G_{12}} \tag{9}$$

$$\frac{1}{G_{xy}}=\frac{4c\cos^2\theta\sin^2\theta}{E_1}\left(1+\upsilon_{12}\right)+\frac{4c\cos^2\theta\sin^2\theta}{E_2}\left(1+\upsilon_{21}\right)+\frac{\left(\cos^2\theta-\sin^2\theta\right)^2}{G_{12}} \tag{10}$$

$$\frac{\upsilon_{xy}}{E_x}=\frac{\upsilon_{yx}}{E_y}=\frac{\cos^2\theta}{E_1}\left(\cos^2\theta\upsilon_{12}-\sin^2\theta\right)+\frac{\sin^2\theta}{E_2}\left(\sin^2\theta\upsilon_{21}-\cos^2\theta\right)+\frac{\cos^2\theta\sin^2\theta}{G_{12}} \tag{11}$$

The properties of the lamina along the plate geometrical axes for the three different fiber orientations and for each of the three fiber volume fractions are estimated using the equations 8 to 11 and are tabulated as shown in Table 3.

Table 3: Mechanical properties of lamina along the plate geometry reference axes

Property	**Volume Fraction V_f=0.75**			**Volume Fraction V_f=0.5**			**Volume Fraction V_f=0.25**		
	θ=0dg	**θ=45dg**	**θ=90dg**	**θ=0dg**	**θ=45dg**	**θ=90dg**	**θ=0dg**	**θ=45dg**	**θ=90dg**
E_x (Gpa)	177.32	17.83	10.41	119.65	10.636	7.594	61.975	6.897	5.682
E_y(Gpa)	10.41	17.83	177.32	7.594	10.636	119.65	5.682	6.897	61.975
G_{xy}(Gpa)	7.98	9.58	7.98	4.155	6.913	4.155	2.513	4.945	2.513
υ_{xy}	0.2375	0.1173	0.01394	0.275	0.311	0.01745	0.312	0.3722	0.0286
υ_{yx}	0.01394	0.1173	0.2375	0.01745	0.311	0.275	0.0286	0.3722	0.312

The stress concentration around the hole of the lamina due to the applied far field unidirectional uniform stress along the longitudinal axis of the plate geometry for the three different fiber orientations and for each of the three fiber volume fractions is estimated using the H.J.Konish relation and Whitney-Nuismer equation as given below.

$$\sigma_{max}=\sigma\left(1+\frac{1}{2}\rho^{-2}+\frac{3}{2}\rho^{-4}-\left(\frac{k-3}{2}\right)\left(5\rho^{-6}-7\rho^{-8}\right)\right) \text{ (H.J.Konish)} \tag{12}$$

σ_{max} is the max stress intensity around the hole vicinity.

σ is the far field uniform stress applied along the geometric longitudinal axis of plate.

$\rho=\frac{y}{a}$ (Ratio of distance along the in plane transverse axis of hole to the hole radius)

k is the stress concentration factor given by Whitney-Nuismer equation as shown below.

$$k = 1 + \sqrt{\left(\frac{2}{A_{yy}}\left(\sqrt{A_{xx}A_{yy}} - A_{xy} + \left(\frac{A_{xx}A_{yy} - A_{xy}^2}{A_{ss}}\right)\right)\right)} \quad \text{(Whitney-Nuismer)} \tag{13}$$

Where A_{xx}, A_{yy}, A_{xy} and A_{ss} are the in plane extension stiffness components and are expressed as :

$$A_{xx} = \sum_{k=1}^{n} (Q_{xx})_k (Z_k - Z_{k-1}) \tag{14}$$

$$A_{yy} = \sum_{k=1}^{n} (Q_{yy})_k (Z_k - Z_{k-1}) \tag{15}$$

$$A_{xy} = \sum_{k=1}^{n} (Q_{xy})_k (Z_k - Z_{k-1}) \tag{16}$$

$$A_{ss} = \sum_{k=1}^{n} (Q_{ss})_k (Z_k - Z_{k-1}) \tag{17}$$

Where Q_{xx}, Q_{yy}, Q_{xy} and Q_{ss} are the in plane stffnesses with reference to the geometrical axes of the lamina under consideration. k=1 to n denotes the number of layers and Z_k , Z_{k-1} are the layer thicknesses measured from the mid plane of the laminate. For the present problem, since there is only a single layer, Z_{k-1}=0, Z_k represents one half of the layer thickness and the number of layers n=1. The stffnesses along the plate geometrical axes are obtained by transforming the stffnesses along the material (fiber) directions using the following transformation equations.

$$Q_{xx} = Q_{11}\cos^4\theta + Q_{22}\sin^4\theta + 2(Q_{12} + 2Q_{66})\sin^2\theta\cos^2\theta \tag{18}$$

$$Q_{yy} = Q_{11}\sin^4\theta + Q_{22}\cos^4\theta + 2(Q_{12} + 2Q_{66})\sin^2\theta\cos^2\theta \tag{19}$$

$$Q_{xy} = (Q_{11} + Q_{22} - 4Q_{66})\sin^2\theta\cos^2\theta + Q_{12}(\cos^4\theta + \sin^4\theta) \tag{20}$$

$$Q_{ss} = (Q_{11} + Q_{22} - 2Q_{12} - 2Q_{66})\sin^2\theta\cos^2\theta + Q_{66}(\cos^4\theta + \sin^4\theta) \tag{21}$$

The stffnesses along the material (fiber) direction are expressed in terms of lamina properties as shown:

$$Q_{11} = \frac{E_1}{1 - \upsilon_{12}\upsilon_{21}} \tag{22}$$

$$Q_{22} = \frac{E_2}{1 - \upsilon_{12}\upsilon_{21}} \tag{23}$$

$$Q_{12} = \frac{\upsilon_{12}E_2}{1 - \upsilon_{12}\upsilon_{21}} \tag{24}$$

$$Q_{66} = G_{12} \tag{25}$$

The maximum stress intensity around the hole vicinity given by equation 12 is estimated for different hole sizes, fiber volume fractions and for different fiber orientations using equations 13 to 25.

Finite Element Analysis

The plate geometry considered has the dimensions (Length=200mm, Width=100mm and thickness=5mm). It is modeled as a single layered composite lamina having centrally placed hole using the Shell99 layered element available in the ANSYS10 element library. The shell99 element coordinate system is initially reoriented in such a way that the shell99 element normals are parallel to the Z-axis of the global Cartesian coordinate system. The plate is modeled in such a way that the length of the plate remains parallel to the reference x-axis of ANSYS coordinate system. The plate is modeled with an element edge length of 4mm for all the sides of the plate and with 10 elements on each quarter of the hole. The plate is loaded by arresting all the degrees of freedom along the left edge of the plate and by applying a uniform pressure intensity of 10Mpa on the right edge. Figure 1 shows the finite element model of the plate with fine mesh around the hole vicinity.

Results and Discussion

The maximum stress intensity around the hole vicinity for different hole sizes, fiber volume fractions and fiber orientations obtained from theory and finite element analysis are tabulated in Tables 4 to 6.

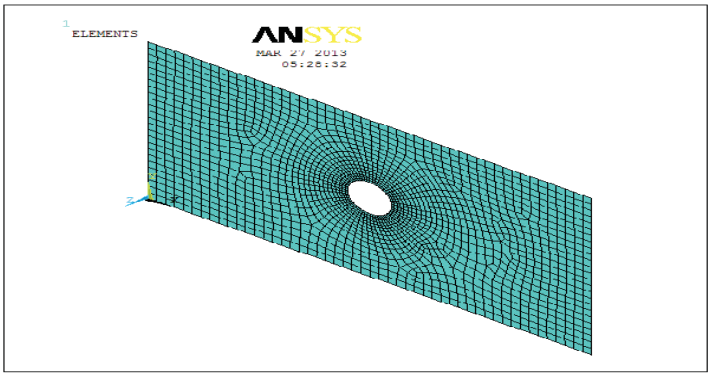

Figure 1: Meshed plate with fine mesh around the hole vicinity

Table 4. Max stress intensity around the hole vicinity for hole diameter equal to 10mm

Max Stress	**V_f=0.75**			**V_f=0.5**			**V_f=0.25**		
(Mpa)	**θ=0dg**	**θ=45dg**	**θ=90dg**	**θ=0dg**	**θ=45dg**	**θ=90dg**	**θ=0dg**	**θ=45dg**	**θ=90dg**
Theory	27.943	18.054	12.985	28.012	17.021	13.885	26.914	19.012	15.007
Ansys	25.665	16.112	11.783	26.510	15.985	12.651	25.493	17.599	13.378

Table 5. Max stress intensity around the hole vicinity for hole diameter equal to 20mm

Max Stress	V_f=0.75			V_f=0.5			V_f=0.25		
(Mpa)	θ=0dg	θ =45dg	θ =90dg	θ =0dg	θ=45dg	θ=90dg	θ =0dg	θ=45dg	θ=90dg
Theory	30.022	19.345	14.111	33.022	21.854	16.847	29.454	21.566	17.654
Ansys	28.664	17.29	12.485	31.432	20.012	15.421	27.198	19.022	15.985

Table 6. Max stress intensity around the hole vicinity for hole diameter equal to 30mm

Max Stress	V_f=0.75			V_f=0.5			V_f=0.25		
(Mpa)	θ=0dg	θ =45dg	θ =90dg	θ =0dg	θ=45dg	θ=90dg	θ =0dg	θ=45dg	θ=90dg
Theory	35.987	25.777	17.111	38.022	27.861	22.041	41.764	31.366	24.974
Ansys	33.019	22.568	15.687	36.432	26.019	19.231	39.789	29.087	22.125

Figures 2 to 4 show the stress distribution around the vicinity of holes of different sizes, for volume fraction (V_f=0.75) and for fiber orientation (θ=0deg).

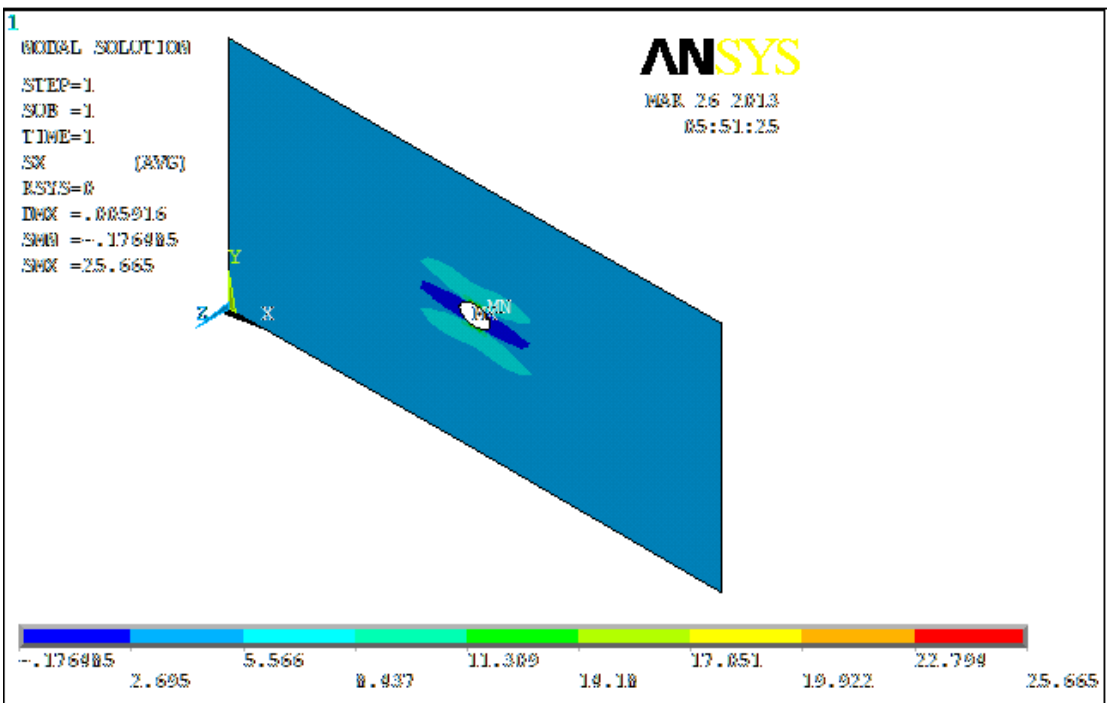

Figure 2: Stress Intensity around hole vicinity for hole of 10mm diameter for V_f=0.75 and q =0dg.

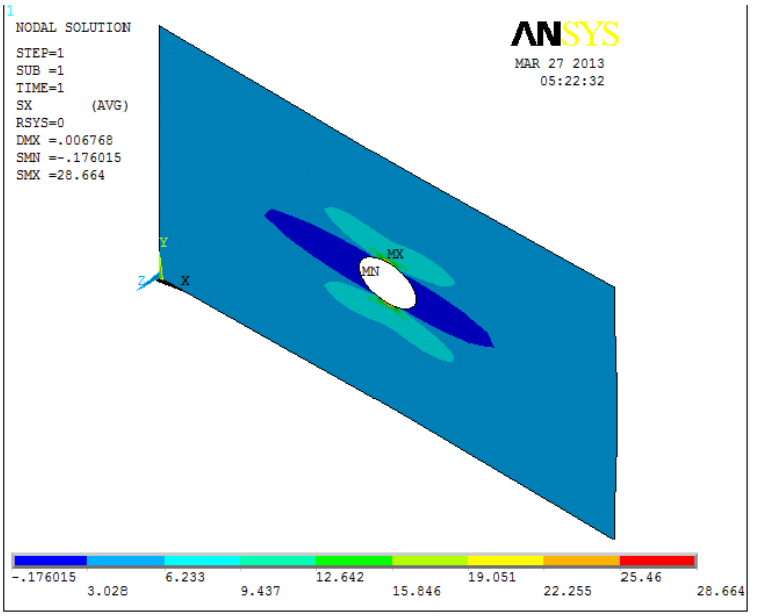

Figure 3: Stress Intensity around hole vicinity for hole of 20mm diameter for V_f=0.75 and q =0dg.

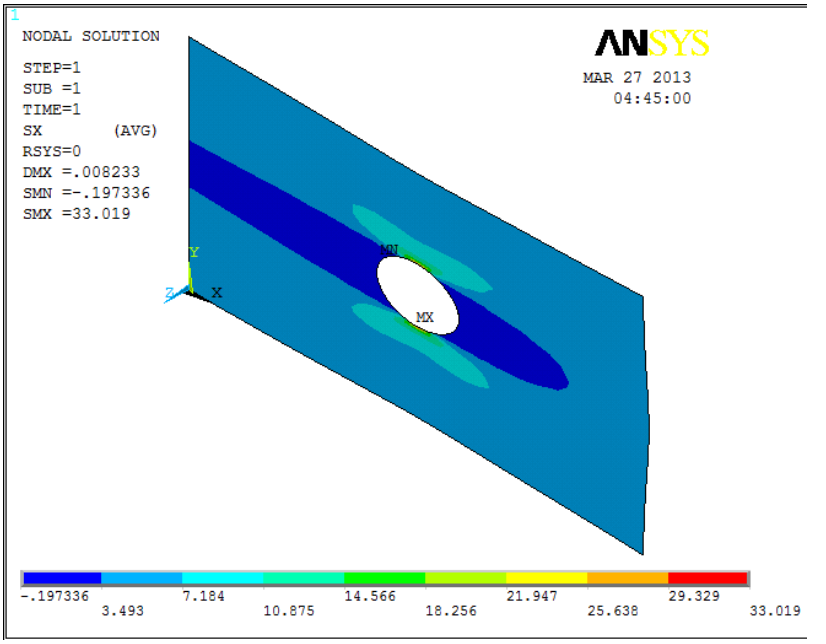

Figure 4: Stress Intensity around hole vicinity for hole of 30mm diameter for V_f=0.75 and q =0dg.

Figure 5 shows the variation in stresses for different hole sizes, different fiber angles and for volume fraction (V_f=0.75). Figure 6 shows the variations in stresses for different fiber volume fractions, for a specified fiber angle and for a given hole size. Figure 7 shows the variation in stresses for a given hole size, for different fiber angles and for a given volume fraction (V_f=0.75).

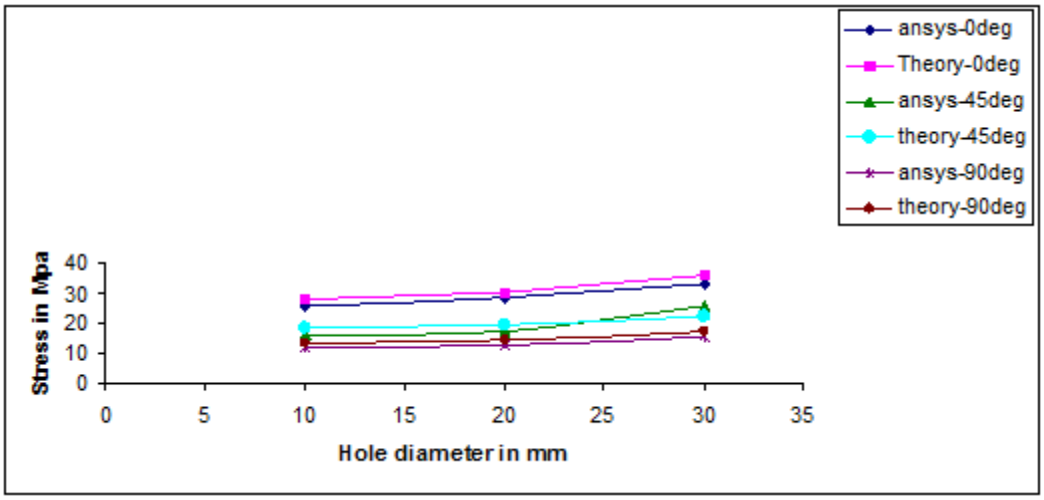

Figure 5: Variation of stress with hole size for different fiber angles (Volume fraction V_f=0.75)

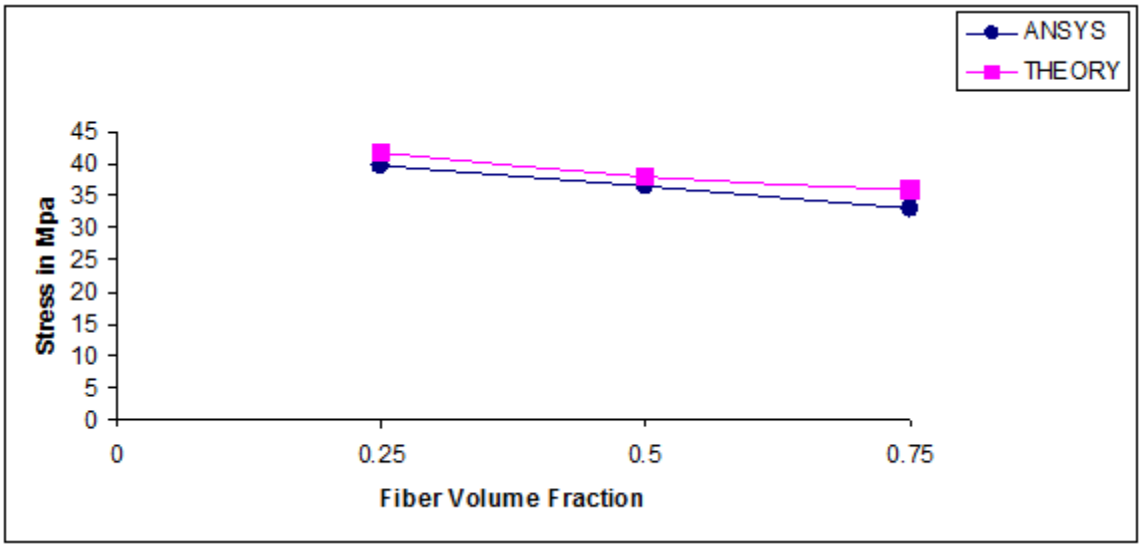

Figure 6: Stress variation with fiber volume fraction for hole D =30mm and fiber angle q =0deg.

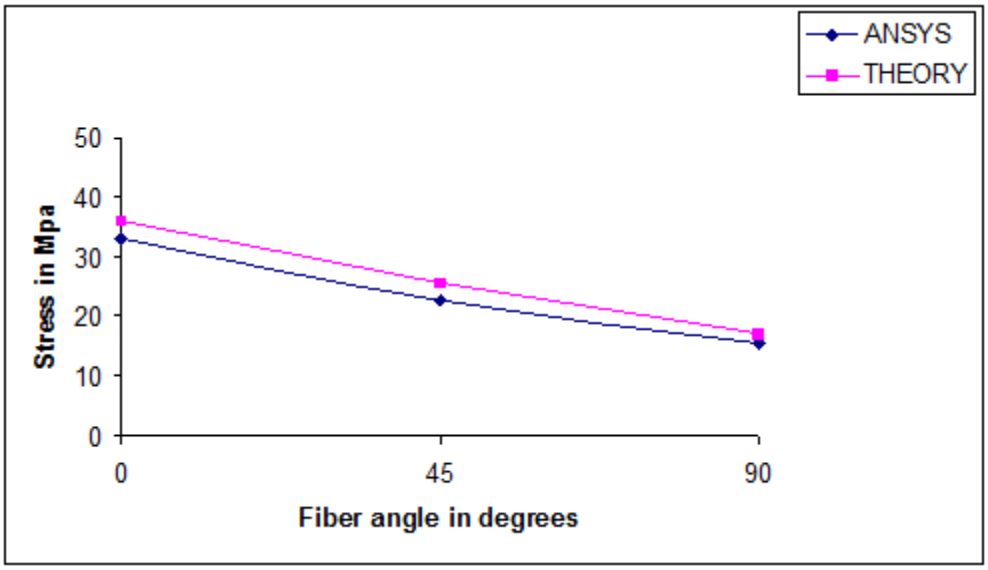

Figure 7: Variation of stress with fiber angle for hole D=30mm and volume fraction V_f=0.75

From tables 4 to 6 and figures 5 to 7, it can be observed that the fiber angle has the most significant influence on stress variation around the hole vicinity followed by hole size and fiber volume fraction. The impact of fiber angle and hole size on stress intensity distribution around the hole can be explained from the illustrated figures A, B and C.

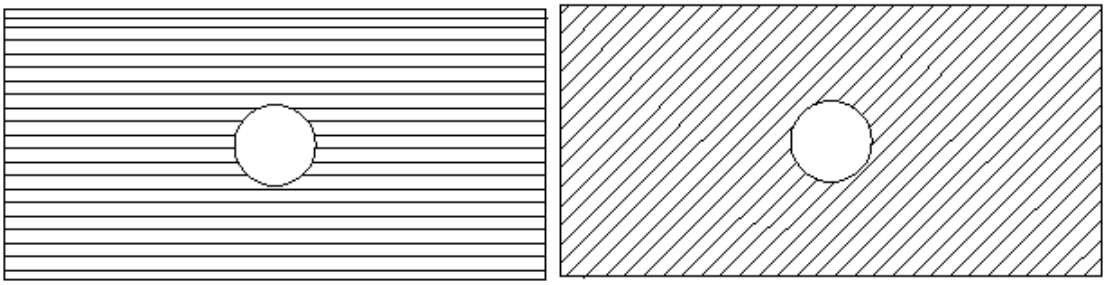

Figure A: Two different fiber orientations for a given hole size and fiber volume fraction

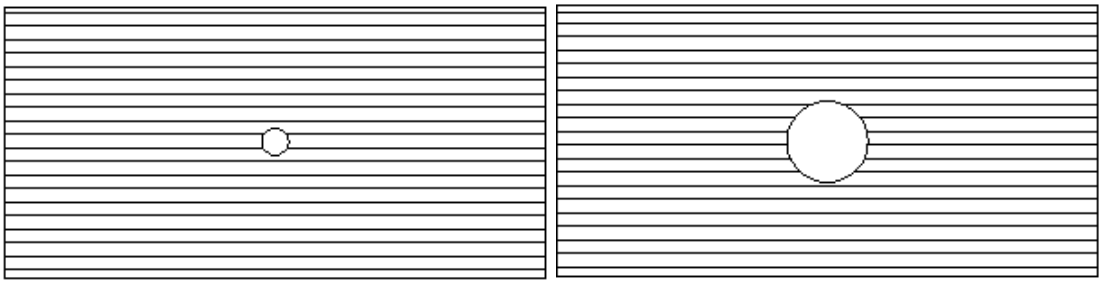

Figure B: Two different hole sizes for a given fiber angle and fiber volume fraction

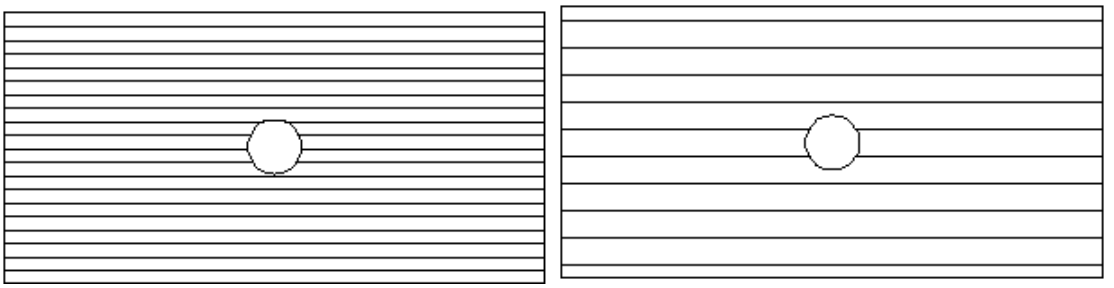

Figure C: Two different fiber volume fractions for a given hole size and fiber angle

At θ =0 deg, large portion of the load is carried by the fibers. Maximum stress intensity arises around the discontinuous fiber region of the hole vicinity, as the number of continuous fibers along the in plane transverse section near the hole sharing the load decreases. At θ =90 deg, the maximum load intensity is taken by the matrix phase. But at fiber angle θ =45 deg as shown in figure A, the fibers will also be subjected to shear stress due to a high probability of slippage at the fiber-matrix interface apart from the normal tensile component of stress resulting in high stress intensity distribution around the hole vicinity. As the hole diameter increases as shown in figure B, the number of discontinuous fibers increases followed by a large discontinuous matrix region. This creates a high magnitude of stress around the continuous fibers and matrix region close to the hole vicinity. It can be seen from figure C that the number of fibers sharing the far field uniformly applied stress intensity varies. Under unidirectional loading with fibers parallel to the applied load, the major portion of the load is carried by fibers. However, for low fiber volume fractions the portion of load shared by the matrix phase also increases. This to some extent compensates for the load portion to be shared by the continous fibers near the hole vicinity.

Conclusions

The present work analyzed the influence of fiber angle, hole size and fiber volume fraction on the stress concentration around the circular hole of an orthotropic lamina using theoretical and finite element approaches. At the fiber angle θ =0deg, hole diameter D=30mm and for a fiber volume fraction V_f=0.25, the stress concentration intensity around the hole neighborhood is found to be maximum. Unlike fiber angle and hole size, the independent variation of fiber volume fraction did not have any significant influence on the stress intensity distribution around the hole vicinity.

Nomenclature

E_{1f} : Longitudinal fiber Elastic modulus (Gpa).
E_m : Matrix Elastic modulus (Gpa).
G_m : Matrix shear modulus (Gpa).
V_m : Matrix volume fraction.
ξ : Fiber packing Parameter.

υ_{12f} : Fiber major Poisson's ratio.

E_{2f} : Transverse fiber Elastic modulus (Gpa).
G_{12f} : Fiber Shear modulus (Gpa).
V_f : Fiber volume fraction.
η : shear modulii ratio.
θ : Fiber orientation w.r.t plate geometric axes in degrees.
υ_m : Matrix Poisson's ratio.

Subscripts

x,y : Directions along and perpendicular to plate geometry.

1,2 : Directions along the length of the fibers and transverse to the length of fibers.

References

B.T. Astrom, 1992, "Manufacturing of polymer composites", Chapman and Hall Publications, London.

C.T. Sun, 2000, "Strength analysis of unidirectional composites and laminates", in comprehensive composite materials, A. Kelly and C.Zweben edition, chapter 1.20, Elsevier Science Ltd., oxford.

H.J. Konish and J.M. Whitney, 1975, "Approximate stresses in an orthotropic plate containing a circular hole", *Journal of Composite Materials*, **9**:157-166.

I.M. Daniel, R.E. Rowlands and J.B.Whiteside, 1974, "Effects of material and stacking sequence on behaviour of composite plates with holes", *Journal of Experimental Mechanics*, **14**:1-9.

I.M. Daniel, 1982, "Failure mechanisms and fracture of composite laminates with stress concentrations", proceedings of seventh international conference on experimental stress analysis, Israel, pp:1-20.

J.C. Halpin and S.W. Tsai, 1967, "Effects of environmental factors on composite materials", Airforce technical Report AFML-TR-67-423, Wright Aeronautical labs, Dayton, OH.

J.C. Halpin, 1969, "Stiffness and expansion estimates for oriented short fiber composites", *Journal of Composite Materials*, **3**:732-734.

J. Awerbuch and M.S. Madhukar, 1985, "Notched strength of composite laminates; predictions and experiments"-A Review, *Journal of Reinforced Plastics and Composites*, **4**:3-159.

O. Ishai, 1971, "Failure of unidirectional composites in tension", *J. Eng. Mech. Div.*, **97**:205-221.

P.K. Mallick, 1993, "Fiber reinforced composites: materials, manufacture and design", Marcel-Dekker, IInd edition.

R.J. Nuismer and J.M. Whitney, 1975, "Uniaxial failure of composite laminates containing stress concentrations", in fracture mechanics of composites, ASTM STP 953, American society for testing materials, pp:117-142.

R.F. Karlak, 1977, "Hole effects in a related series of symmetrical laminates", proceedings in failure modes in composites, The metallurgical society of AIME, chicago, **IV**:105-112.

S.W. Tsai and E.M.Wu, 1971, "A general theory of strength of anisotropic materials", *Journal of Composite Materials*, **5**:58-80.

Z. Hashin, 1983, "Analysis of composite materials-A Survey", ASME *Journal of Applied Mechanics*, **50**: 481-505.